# Short Papers

## 3-D Locomotive and Drilling Microrobot Using Novel Stationary EMA System

Hyunchul Choi, Kyoungrae Cha, Semi Jeong, Jong-oh Park, and Sukho Park

***Abstract*—For 3-D locomotion and drilling of a microrobot, we proposed an electromagnetic actuation (EMA) system consisting of three pairs of stationary Helmholtz coils, a pair of stationary Maxwell coils, and a pair of rotating Maxwell coils in the previous research [1]. However, this system could have limited medical applications because of the pair of rotational Maxwell coils. In this paper, we propose a new EMA system with three pairs of stationary Helmholtz coils, a pair of stationary Maxwell coils, and a new locomotive mechanism for the same 3-D locomotion and drilling of the microrobot as achieved by the previously proposed EMA system. For the performance evaluation of the proposed EMA system, we perform a 3-D locomotion and drilling test in a blood vessel phantom. In addition, the two EMA systems are compared to show that the newly proposed EMA system has 440% wider working space and 49% less power consumption than the previous EMA system.**

***Index Terms*—Drilling and locomotion, electromagnetic, Helmholtz coil, intravascular, microrobot, Maxwell coil.**

### I. Introduction

Recently, minimal invasive surgery (MIS) has become the focus of interest in medical treatment because of short operation time, short recovery period, and minimal scarring. As a possible solution of MIS, microrobots have become the subject of much research. A potential medical innovation, the microrobot can access narrow and unreachable regions of the human organ [2]. However, due to the size limitation of the microrobot, the actuation part, including the power source, has been difficult to integrate into the microrobot body [3]. To solve this problem, many researchers have developed various magnetic actuating methods for the locomotion and drilling of a microrobot [1]–[17]. The microrobots actuated by magnetic fields were used as therapeutic tools of eyeball and blood vessel, diagnostic devices of capsule endoscope, and manipulation methods of cell or microparticles.

Nelson *et al.* proposed the OctoMag system with eight electromagnets, which precisely controlled the current of the electromagnetic coils to enable a microrobot to realize 5-DOF motion [4]. Nelson and Arai groups proposed a locomotion mechanism that uses a rotational magnetic field to move a microrobot with a spiral-shaped body [5], [6]. The EMA system with three pairs of stationary Helmholtz coils rotates the spiral body and propels it. Martel *et al.* proposed a 3-D locomotion mechanism for a ferromagnetic core using the conventional magnetic resonance imaging system [7]. With this system, the microrobot could move and position track simultaneously. Sitti *et al.* suggested a microrobot with stick-slip motion by their proposed EMA system and used it for the manipulation of microparticle [8]. Dario *et al.* proposed a robotic magnetic steering and locomotion of capsule endoscope using an external permanent magnet attached on a multi-axis robot [9].

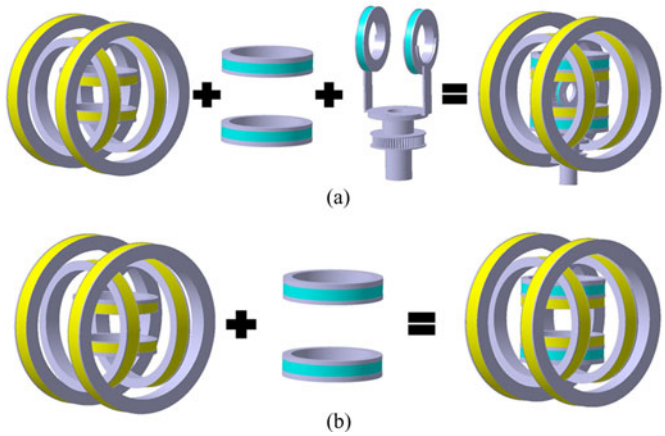


Fig. 1. Coil structures of EMA systems. (a) Previous EMA system has three pairs of stationary Helmholtz coils, a pair of stationary Maxwell coils, and a pair of rotating Maxwell coils. (b) Proposed EMA system has three pairs of stationary Helmholtz coils and a pair of stationary Maxwell coils.

We had proposed 2-D and 3-D locomotive microrobots using EMA systems without drilling function [10], [11]. In addition, we had realized the 3-D locomotion and drilling of a microrobot by using an EMA system with three pairs of stationary Helmholtz coils, a pair of stationary Maxwell coils, and a pair of rotating Maxwell coils, as shown in Fig. 1(a) [1]. Because of the pair of rotating Maxwell coils, however, the EMA system has a relatively small working volume, making it inappropriate for medical application.

Therefore, in this paper, we propose a new EMA system with three pairs of stationary Helmholtz coils and a pair of stationary Maxwell coils, but without the pair of rotational Maxwell coils, as shown in Fig. 1(b). Without the rotating Maxwell coils, the proposed EMA system would have a larger working volume and lower power consumption. To achieve the similar 3-D locomotion and drilling of the microrobot driven by the former EMA system with the pair of rotating Maxwell coils, the new EMA system was operated by a suitable actuation algorithm.

Recently, we have proposed a spiral-shaped microrobot with the similar rotational magnetic EMA coil structure in Fig. 1(b), which has simultaneous locomotion and drilling functions by a rotational magnetic field [12]. In addition, the additive Maxwell coil in EMA system could enhance the propelling and drilling force of the spiral microrobot. The spiral microrobot is rotated by the rotational magnetic field and shows propulsion and drilling motion in the 2-D plane. However, this paper proposed a sphere-shaped microrobot with bumped surface, which separately shows a propulsion motion by a gradient magnetic field and a drilling motion by a rotational magnetic field in 3-D space.

This paper is organized as follows. First, we propose a new EMA system and explain the working principle of the 3-D locomotion and

Manuscript received February 22, 2012; accepted May 19, 2012. Date of publication July 6, 2012; date of current version January 18, 2013. Recommended by Technical Editor D. G. Caldwell. This work was supported by Grant-in-Aid for Strategy Technology Development Programs under Grant 10030037 from the Korea Ministry of Knowledge Economy.

H. Choi, S. Jeong, J. Park, and S. Park are with the Robot Research Initiative, School of Mechanical Engineering, Chonnam National University, Gwangju 500-757, Korea (e-mail: anubis_jjang@hanmail.net; semi0111@gmail.com; jop@jnu.ac.kr; spark@jnu.ac.kr).

K. Cha is with the Daegu Gyeongbuk Medical Innovation Foundation, Daegu 706-010, Korea (e-mail: orotham@dgmif.com).

Color versions of one or more of the figures in this paper are available online at http://ieeexplore.ieee.org.

Digital Object Identifier 10.1109/TMECH.2012.2201494

drilling motion of the microrobot applied with the new EMA system. For accurate 3-D locomotion, the gravitational force of the microrobot is compensated. Second, to verify the performance of the new EMA system, the 3-D locomotion and drilling of a microrobot with the new EMA system are tested in a blood vessel phantom. Finally, the proposed EMA system is evaluated by comparison with the previous EMA system.

## II. Actuation Principle of the Proposed EMA System

### A. Theory of Helmholtz and Maxwell Coils

Generally, an EMA system uses the uniform magnetic field of Helmholtz coils to align the microrobot [1], [13]. The magnetic field ($\mathbf{H}_h$) produced by a pair of $x$-axis Helmholtz coils is described as follows [13]:

$$\mathbf{H}_h = \begin{bmatrix} 0.716\frac{i_h \times n}{r_h} & 0 & 0 \end{bmatrix}^T \tag{1}$$

where $i_h$, $n$, and $r_h$ are the current, the number of turns, and the radius of the Helmholtz coils, respectively. The three pairs of Helmholtz coils generate uniform magnetic-field intensity along the desired direction in the region of interest to align the microrobot also in that direction.

Generally, Maxwell coils are used to generate a uniform gradient magnetic field, which provides the propulsion force of the microrobot. The magnetic field $\mathbf{H}_m$ generated by a pair of $z$-axis Maxwell coils is expressed as follows [13]:

$$\mathbf{H}_m = [-0.5 g_m x \quad -0.5 g_m y \quad g_m z]^T \tag{2}$$

$$g_m = 0.641\frac{i_m \times n}{r_m^2} \tag{3}$$

where $g_m$ denotes the gradient of the magnetic field produced by the $z$-axis Maxwell coils and $x$, $y$, and $z$ are the coordinates of each axis. In addition, $i_m$, $n$, and $r_m$ are the current, the number of turns, and the radius of the Maxwell coils, respectively.

### B. Alignment and Propulsion of Microrobot for Locomotion

For 3-D locomotion of the microrobot, the microrobot should be aligned and propelled along the desired direction. Therefore, first, the three pairs of Helmholtz coils on $x$-, $y$-, and $z$-axis align the microrobot along the desired direction. As shown in Fig. 2, the magnetic-field vector $\mathbf{B}$ by the Helmholtz coils, which aligns the microrobot in 3-D space, can be defined as

$$\mathbf{B} = \begin{bmatrix} B_x \\ B_y \\ B_z \end{bmatrix} = \begin{bmatrix} B\cos\alpha\cos\beta \\ B\sin\alpha\cos\beta \\ -B\sin\beta \end{bmatrix} \tag{4}$$

where $B$ is the magnetic flux density, $B_x$, $B_y$, and $B_z$ are the magnetic field components along the three axes, respectively, $\alpha$ is the alignment angle in the $x$–$y$ plane, and $\beta$ is clockwise rotation angle from the $r$-axis in the $r$–$z$ plane. Magnetization $\mathbf{M}$ of the microrobot can be expressed as follows:

$$\mathbf{M} = \begin{bmatrix} M_x \\ M_y \\ M_z \end{bmatrix} = \begin{bmatrix} M\cos\alpha\cos\beta \\ M\sin\alpha\cos\beta \\ -M\sin\beta \end{bmatrix} \tag{5}$$

where $M$ is the resultant magnetization of the microrobot, $M_x$, $M_y$, and $M_z$ are the magnetization intensity components along the three axis, respectively.

Second, the propulsion mechanism of the microrobot in the proposed EMA system is described in Fig. 3. In order to generate the propulsion

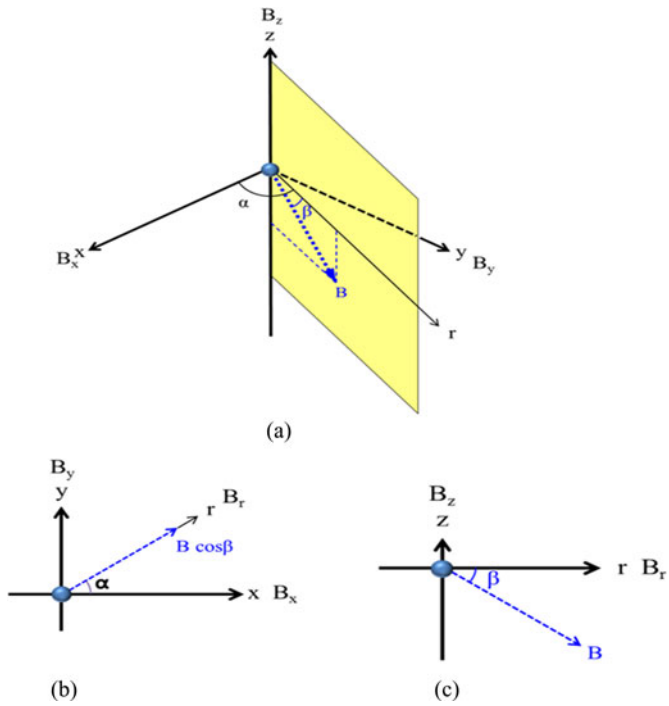


Fig. 2. Alignment of the microrobot in the 3-D space. (a) Cartesian coordinate system. (b) $x$–$y$ plane. (c) $r$–$z$ plane.

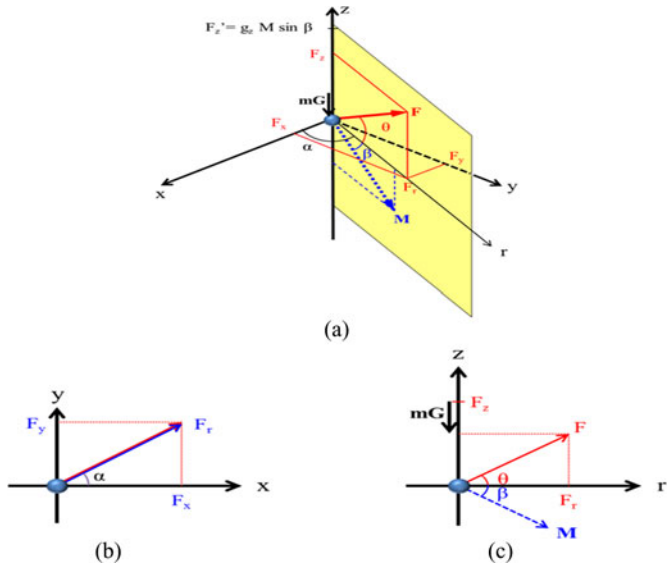


Fig. 3. Propulsion of the microrobot in the 3-D space. (a) Cartesian coordinate system. (b) $x$–$y$ plane. (c) $r$–$z$ plane.

force of the microrobot in 3-D space, the propulsion force vector $\mathbf{F}$ denoted in Fig. 3(b) and (c) can be described as

$$\mathbf{F} = \begin{bmatrix} F_x \\ F_y \\ F_z \end{bmatrix} = \begin{bmatrix} F\cos\alpha\cos\theta \\ F\sin\alpha\cos\theta \\ F\sin\theta + mG \end{bmatrix} \tag{6}$$

where $F$ is the propulsion force, $F_x$, $F_y$, $F_z$ are the propulsion force components along the three axes, respectively, $\alpha$ is the alignment and

propulsion angle in the $x$–$y$ plane, and $\theta$ is the counter clockwise propulsion angle from the $r$-axis in the $r$–$z$ plane. Generally, the alignment angle $\beta$ in (4) and the propulsion force direction $\theta$ in (6) are not the same. For more precise locomotion in 3-D space, the gravitational force $mG$ of the microrobot is considered.

The Maxwell coils of the proposed EMA system are used to generate the propulsion force, as expressed in (6). If a reverse current was applied to the $z$-axis Maxwell coils, the magnetic field of (2) can be rewritten as

$$\mathbf{H}_m = [0.5g_z x \quad 0.5g_z y \quad -g_z z]^T. \tag{7}$$

If the alignment direction of the microrobot ($\alpha$, $\beta$) and the gradient magnetic field generated by the $z$-axis Maxwell coils are considered, the propulsion force of the microrobot can be described as

$$\mathbf{F} = \begin{bmatrix} F_x \\ F_y \\ F_z \end{bmatrix} = \begin{bmatrix} 0.5g_z MV\cos\alpha\cos\beta \\ 0.5g_z MV\sin\alpha\cos\beta \\ g_z MV\sin\beta \end{bmatrix}. \tag{8}$$

Generally, the volume $V$ and the magnetization $M$ of the microrobot are considered as known constant values. Therefore, the propulsion force of the microrobot along the desired direction can be determined if the alignment angle $\beta$ and the magnetic gradient $g_z$ of the $z$-axis Maxwell coils are known. From (6) and (8), the following relational equations can be derived:

$$g_z MV = \frac{2F\cos\theta}{\cos\beta} \tag{9}$$

$$g_z MV\sin\beta = F\sin\theta + mG. \tag{10}$$

Based on the relations of (9) and (10), the alignment angle $\beta$ and the magnetic gradient $g_z$ can be obtained as

$$\beta = \tan^{-1}\left(\frac{F\sin\theta + mG}{2F\cos\theta}\right) \tag{11}$$

$$g_z = \frac{F\sin\theta + mG}{MV\sin\left(\tan^{-1}\left(F\sin\theta + mG/2F\cos\theta\right)\right)}. \tag{12}$$

The alignment direction of the microrobot $\alpha, \beta$ and the magnetic gradient $g_z$ by the $z$-axis Maxwell coils can be obtained from (11) and (12) to determine the propulsion force of the microrobot along the desired direction $\alpha, \theta$.

### C. Rotation of Microrobot for Drilling

Through the alignment and propulsion mechanisms in the previous section, the microrobot reaches the target occlusion. To treat the occlusion, the microrobot can drill into it by rotating its body along the desired axis.

First, the magnetization direction can be expressed with $\alpha$ and $\beta$ in Fig. 3(a). Second, the microrobot rotates about the desired axis (rotational axis), which is perpendicular to the direction of magnetization. For the rotational motion, the magnetic fields from the three axes Helmholtz coils can be described as

$$\mathbf{B} = \begin{bmatrix} B_x(t) \\ B_y(t) \\ B_z(t) \end{bmatrix} = \begin{bmatrix} B_0\cos\alpha\cos(\varpi t) \\ B_0\sin\alpha\cos(\varpi t) \\ -B_0\sin(\varpi t) \end{bmatrix} \tag{13}$$

where $B_0$ is the magnetic-field intensity of the Helmholtz coils and $\varpi$is the rotational frequency of the microrobot. Based on (13), the microrobot can be rotated to drill into the occlusion.

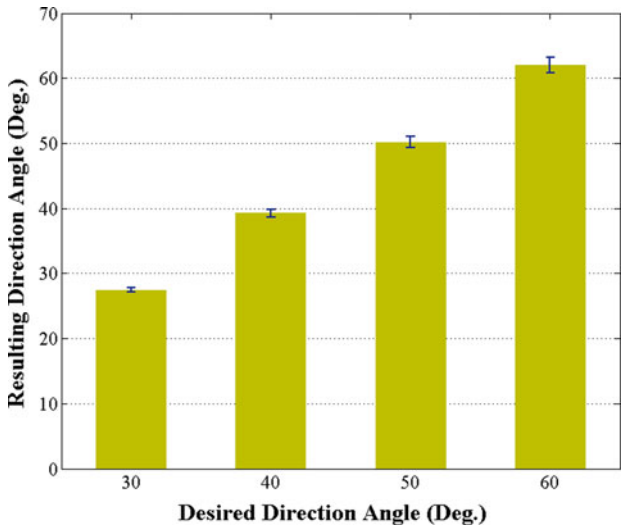


Fig. 4. Experimental results of basic locomotion tests.

## III. Experiments

### A. EMA Coil System and Microrobot

The structure of proposed EMA system used in the experiment is shown in Fig. 1(b). The new EMA system was constructed by eliminating the pair of rotational Maxwell coils that were used in the previous EMA system [1]. In the basic locomotion test, a cylinder type permanent magnet of 2-mm diameter and 2-mm length was used to measure the magnetization direction and the propulsion direction. In addition, for the locomotion and the drilling in the phantom of a blood vessel, we used the same sphere type microrobot with a bumpy surface, which was fabricated in the previous research [1].

### B. Basic Locomotion Tests

We tested the tracking performance of the microrobot in the desired directions in an acrylic test cube (20 mm × 10 mm × 20 mm), which was filled with high-viscosity silicone oil (100 cP). For the basic experiments, we selected $\alpha = 90°$ ($y$–$z$ plane), which means that the microrobot should move along the desired directions under the gravitational force effect. We executed the locomotion test of the microrobot in four directions ($\theta = 30°$, 40°, 50°, and 60°) in the $y$–$z$ plane and all cases were repeated five times. The tracking angle of the microrobot was measured from the recorded videos, and based on this information, the experimental results were summarized. The tracking results of the microrobot are summarized in Fig. 4. The basic experimental results verified that the microrobot could track the desired directions within the error range of 2°–3°.

### C. 3-D Locomotion and Drilling in the Blood Vessel Phantom

For verification of the 3-D locomotion capability of the microrobot under a condition similar to that of a blood vessel, a blood vessel phantom was used. The phantom was fabricated by rapid prototyping using the data of a rendered vessel obtained from computed tomography images of an actual blood vessel. The vessel of the phantom was filled with high viscous silicone oil (350 cP), and one branch was filled with 0.25% agar as an occlusion model. A spherical microrobot with bumps was used for the locomotion and drilling tests. The locomotion and drilling motion of the microrobot inside the blood vessel phantom were controlled with a joystick controller.

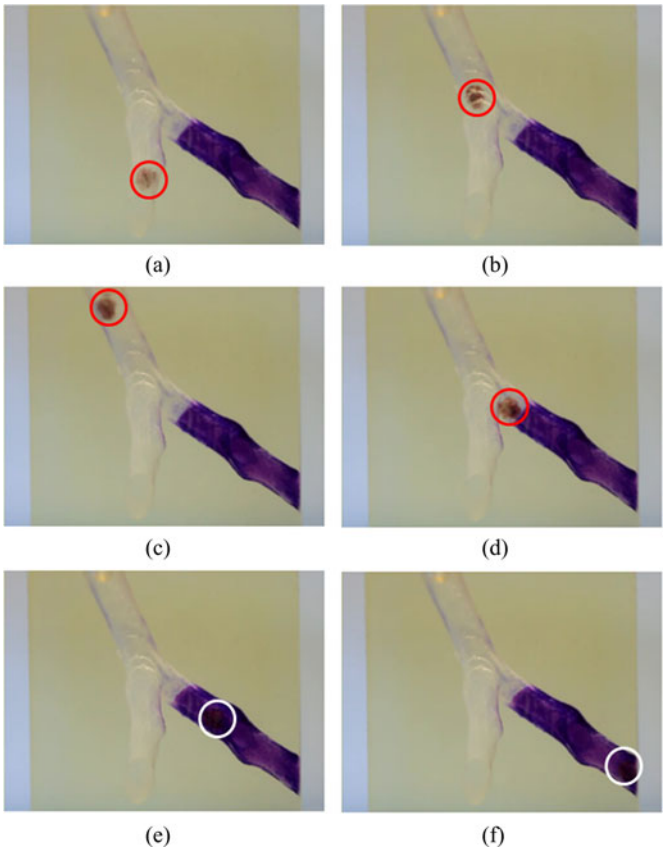


Fig. 5. Locomotion and drilling test of microrobot in blood vessel phantom: (a) 1 s, (b) 12 s, (c) 24 s, (d) 34 s, (e) 140 s, and (f) 148 s.

Fig. 5 shows the experimental result of the locomotion and drilling of the microrobot using the proposed EMA system. The experimental results verified that the microrobot could move about 80 mm in 34 s and drill 20 mm into the agar in 10 s after the microrobot was stuck into the agar.

## IV. Comparison Between Two EMA Systems

The proposed EMA system has the same functions as the previous EMA system [1]. However, the new EMA system has a different EMA coils structure and actuation mechanism. These two EMA systems have the same Helmholtz coils structure but a different Maxwell coils structure; the new EMA system does not have a pair of rotational Maxwell coils but has a pair of $z$-axis stationary Maxwell coils. Therefore, the proposed EMA system is smaller than the previous EMA system, and is actuated by lower electrical power.

In this section, we compare these two EMA systems with respect to working space and power consumption. For a reasonable comparison, the following assumptions [12], [13] are introduced.

1) The distances between all coils are calculated by using design values and the bundle of the coil winding is assumed as a line.
2) The two EMA systems generate locomotion in 3-D space and equally compensate the gravitational force acting on the microrobot. Therefore, in a simple comparison, the gravitational force acting on the microrobot is not considered.
3) Because the gradient magnetic fields of the Maxwell coils can be controlled by changes to the direction of the applied current, the current directions of both EMA systems are not compared, but the absolute values of the currents are compared.

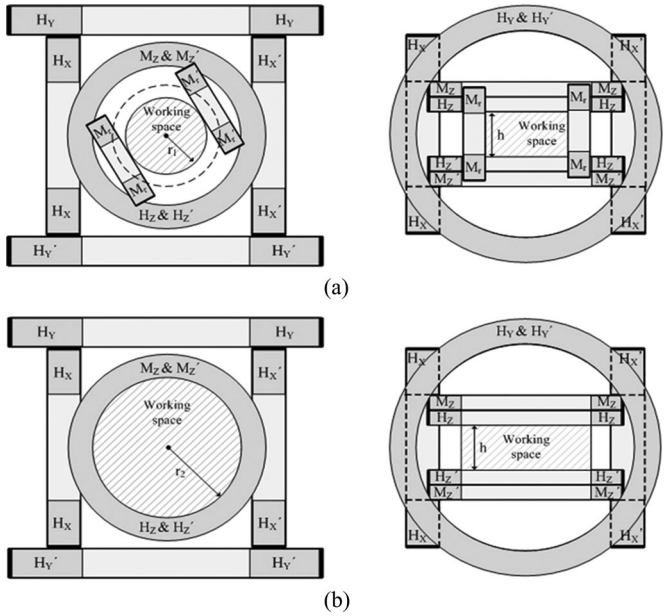


Fig. 6. Working space of the two EMA coil systems: (a) previous EMA system and (b) proposed EMA system.

TABLE I
Comparison of Power Consumption and Working Space Between Two EMA

| | Previous System | | Proposed System |
|---|---|---|---|
| Coil pair | $M_r$ | $M_z$ | $M_z$ |
| Radius | $r$ | $1.814r$ | $1.814r$ |
| Turns | $n$ | $3.291n$ | $3.291n$ |
| Resistance | $2\pi rR$[(1)] | $11.940\pi rR$ | $11.940\pi rR$ |
| Required current | $I$[(2)] | $I$ | $0.594I$ |
| Power consumption | $13.940\pi rnRI^2$ | | $7.098\pi rnRI^2$ |
| Working space | $0.75\pi r^2h$ | | $3.29\pi r^2h$ |

[(1)] $R$ means the resistance per unit length of the coil.
[(2)] $I$ means the average required current for the same propulsion force of the microrobot to the arbitrary direction.

4) All EMA coils have the same wire thickness. Therefore, the resistances of the coils are proportional to their lengths.

First, the working spaces of the two EMA systems, which have similar cylindrical shapes, are compared in Fig. 6. Determined by the distance between the $z$-axis Helmholtz coils, the working spaces of the two EMA systems have the same height. The radius $r_1$ of the previous EMA system was determined by the distance between the rotational Maxwell coils, but the radius $r_2$ of the proposed EMA system was determined by the radius of the $z$-axis Helmholtz coil. Therefore, the new EMA system could have a bigger working space than the previous EMA system. The detail comparison of the working space between the two EMA systems is summarized in Table I.

Second, the power consumption between two EMA systems is compared. The average required currents required to generate the same propulsion force of the microrobot in an arbitrary direction was calculated. In the previous EMA system, the required currents of two

Maxwell coils had to be the same current value of $I$. From the required currents and the resistances of the coils, the power consumptions of two Maxwell coils were calculated and the sum of the power consumptions was the total power consumption of the previous EMA system. The proposed EMA system could propel the microrobot using only the $z$-axis Maxwell coils. For the actuation of the microrobot in arbitrary directions, different coil currents had to be applied. The average required current was calculated as $0.5941I$. By using the average required current and the resistance of the coil, the average power consumption of the proposed EMA system was calculated. The power consumptions between the two EMA systems are described, as shown in Table I.

The new proposed EMA system had 49% less power consumption and 440% bigger working space than the previous EMA system. Consequently, the comparison of the two EMA systems validated that the new proposed EMA system had advantages of a bigger working space and lower power consumption than the previous EMA system.

## V. Conclusion

In the previous research, we proposed an EMA system, which could perform 3-D locomotion and drilling. This EMA system consists of three pairs of stationary Helmholtz coils, a pair of stationary Maxwell coils, and a pair of rotating Maxwell coils. However, because the previous EMA system has a rotational unit and uses two pairs of Maxwell coils, it had a narrow working space and consumed much power. As a solution, the new EMA system, which can perform the same function as the previous EMA system, without the pair of rotational Maxwell coils was introduced in this paper. First, the 3-D locomotion and the drilling mechanism of the microrobot using the proposed EMA system were designed. The actuation mechanism included the compensation algorithm, which compensated the gravitational force of the microrobot. Through basic experiments, we verified the tracking performance of the microrobot using the proposed EMA system, and the actuation mechanism. Second, we verified the 3-D locomotion and the drilling performance of the microrobot using the proposed EMA system in a blood vessel phantom. The microrobot moved about 80 mm in 34 s and drilled into the agar of 20-mm length in 10 s. Finally, by comparison between the new EMA system and the previous EMA system, the new EMA system was found to have 440% bigger working space and 49% less power consumption than the previous EMA system. Consequently, we expect the proposed EMA system to be used for diverse medical applications such as the intravascular microrobot, active drug delivery, and minimal invasive treatment.

## References


[1] C. Yu, J. Kim, H. Choi, J. Choi, S. Jeong, K. Cha, J. Park, and S. Park, "Novel electromagnetic actuation system for 3-D locomotion and drilling of intravascular microrobot," *Sens. Actuators A, Phys.*, vol. 161, no. 1–2, pp. 297–304, Jun. 2010.

[2] B. Nelson, I. Kaliakatsos, and J. Abbott, "Microrobots for minimally invasive medicine," *Annu. Rev. Biomed. Eng.*, vol. 12, pp. 55–85, Aug. 2010.

[3] J. Abbott, Z. Nagy, F. Beyeler, and B. Nelson, "Robotics in the small-part I: Microrobotics," *IEEE Robot. Autom. Mag.*, vol. 14, no. 2, pp. 92–103, Jun. 2007.

[4] M. Kummer, J. Abbott, B. Kratochvil, R. Borer, A. Sengul, and B. Nelson, "OctoMag: An electromagnetic system for 5-DOF wireless micromanipulation," in *Proc. IEEE Int. Conf. Robot. Autom.*, May 2010, pp. 1080–1081.

[5] K. Ishiyama, M. Sendoh, and K. Arai, "Magnetic micromachines for medical applications," *J. Magn. Magn. Mater.*, vol. 242–245, pp. 41–46, Apr. 2002.

[6] L. Zhang, J. Abbott, L. Dong, B. Kratochvil, D. Bell, and B. Nelson, "Artificial bacterial flagella: Fabrication and magnetic control," *Appl. Phys. Lett.*, vol. 94, no. 6, p. 064107, Feb. 2009.

[7] S. Tammz, R. Gourdeau, A. Chanu, J. Mathieu, and S. Martel, "Real-time MRI-based control of a ferromagnetic core for endovascular navigation," *IEEE Trans. Biomed. Eng.*, vol. 55, no. 7, pp. 1854–1863, Jul. 2008.

[8] S. Floyd, C. Pawashe, and M. Sitti, "Microparticle manipulation using multiple untethered magnetic micro-robots on an electrostatic surface," in *Proc. IEEE Int. Conf. Intell. Robots Syst.*, Oct. 2009, pp. 528–533.

[9] G. Ciuti, P. Valdastri, A. Menciassi, and P. Dario, "Robotic magnetic steering and locomotion of capsule endoscope for diagnostic and surgical endoluminal procedures," *Robotica*, vol. 28, pp. 199–207, Oct. 2009.

[10] H. Choi, J. Choi, S. Jeong, C. Yu, J. Park, and S. Park, "Two-dimensional locomotion of a microrobot with a novel stationary electromagnetic actuation system," *Smart Mater. Struct.*, vol. 18, no. 11, pp. 1–6, Sep. 2009.

[11] H. Choi, K. Cha, J. Choi, S. Jeong, S. Jeon, G. Jang, J. Park, and S. Park, "EMA system with gradient and uniform saddle coils for 3D locomotion of microrobot," *Sens. Actuators A, Phys.*, vol. 63, no. 1, pp. 410–417, Sep. 2010.

[12] S. Jeong, H. Choi, K. Cha, J. Li, J. Park, and S. Park, "Enhanced locomotive and drilling microrobot using precessional and gradient magnetic field," *Sens. Actuators A, Phys.*, vol. 171, no. 2, pp. 429–435, Sep. 2011.

[13] S. Jeon, G. Jang, H. Choi, and S. Park, "Magnetic navigation system with gradient and uniform saddle coils for the wireless manipulation of micro-robots in human blood vessels," *IEEE Trans. Magn.*, vol. 46, no. 6, pp. 1943–1946, Jun. 2010.

[14] S. Park and J. Park, "Frontier research program on biomedical microrobot for intravascular therapy," in *Proc. IEEE Biomed. Robot. Biomech.*, Oct. 2008, pp. 360–365.

[15] C. Elbuken, M. Khamesee, and M. Yavuz, "Design and implementation of a micromanipulation system using a magnetically levitated MEMS robot," *IEEE/ASME Trans. Mechatronics*, vol. 14, no. 4, pp. 434–445, Aug. 2009.

[16] M. Mehrtash, N. Tsuda, and M. B. Khamesee, "Bilateral macro–micro teleoperation using magnetic levitation," *IEEE/ASME Trans. Mechatronics*, vol. 16, no. 3, pp. 459–469, Jun. 2011.

[17] Z. Zhang and C.-H. Menq, "Design and modeling of a 3-D magnetic actuator for magnetic microbead manipulation," *IEEE/ASME Trans. Mechatronics*, vol. 16, no. 3, pp. 421–430, Jun. 2011.